A mathematical model for diffusion-induced grain boundary motion

O. Penrose and J.W. Cahn

Abstract. For a film of metallic alloy immersed in a suitable vapour, we use a system of four coupled nonlinear differential equations to model the steady diffusion-induced motion of: a grain boundary, the surfaces of the two grains, and the triple junction where they all meet. One of the equations models diffusion along the moving grain boundary; another models the force balance which determines its speed. The remaining two equations model diffusion in the surfaces of the two grains. The equations are linked by boundary conditions at the triple junction. The resulting system of differential equations and boundary conditions is solved here for the case of 'trailing' grain boundaries (ones where the growing crystal grain develops as a layer beneath the surface of the specimen rather than filling up the entire space between the two surfaces) in a limit where the elastic driving force is very small. The main result is that for small values of Δc, defined as the (experimentally controllable) jump in mole fraction of solute at the triple junction, the growth velocity of the trailing grain is approximately proportional to $(\Delta c)^4$, but for large positive Δc the velocity is approximately proportional to $(\Delta c)^5$. The thickness of the trailing grain is approximately proportional to $(\Delta c)^{-2}$ for small Δc and to $(\Delta c)^{-8/3}$ for large. There is a negative value of Δc beyond which the model predicts that the velocity and thickness are independent of Δc, but this result should be treated with caution because the solution may be unstable.

1. Introduction

Diffusion-induced grain boundary motion (DIGM) was first observed by Hillert and Purdy in 1978 [9]. A thin foil of iron was placed in a vapour of zinc atoms. The zinc diffused along the boundaries between the different crystal grains in the foil, but not into the grains themselves, where the diffusivity is much lower. Parts of these grain boundaries were then observed to move, the grain on one side growing while the grain on the other side shrank. The zinc atoms which had diffused in along the grain boundary were left behind in the newly grown part of the crystal, thereby alloying it. Hillert and Purdy also demonstrated that DIGM occurred for de-alloying by placing a foil of an iron-zinc alloy in a vacuum. DIGM has been observed in many other alloy systems and with many geometries; for a review see ref. [7].

There has been controversy in the metallurgical community about the force that drives DIGM. With a view to helping resolve the controversy, Cahn et al [2] put forward a phase-field model[1] in which the consequences of different assumptions about the driving force could be worked out and compared with experiment. It was concluded that the most likely candidate was a mechanism suggested (in a slightly different context) by Sulonen[14] and first studied quantitatively by Hillert[8]; this mechanism is based on the energy of elastic deformations caused by mismatch between the sizes of the two different types of atom[2]. It remains the only mechanism consistent with all experiments and with some insightful *gedanken* experiments.

The analysis given in ref. [2] is based on the assumption that the grain boundary is flat, but real grain boundaries are not flat: they can curve in the middle while still connecting the two sides of the foil, or they can curve so much that they separate into two parts, one close to each face of the foil. Both types of grain boundary were observed in the original experiments [9]. We shall call them connecting and trailing grain boundaries; they are illustrated in Fig. 1.

To model these curved grain boundaries, Fife et al.[5] developed the mathematics of the phase-field model further, deriving a sharp-interface approximation which led to a system of differential equations for the shape of the grain boundary (represented in this approximation as a geometrical surface). Some numerical studies of both phase-field and sharp-interface models were described at this conference by Vanessa Styles (see also ref. [6]).

2. The equations for the grain boundary

The sharp-interface equations obtained by Fife et al. [5] can also be derived by physical arguments which do not rely on the phase field model [1, 3]. There are two differential equations. One of them, describing diffusion within the grain boundary, can be written (in a specially chosen system of units, *v.i.*)

$$\frac{d^2 c_{gb}}{ds^2} = (c_{gb}(s) - c_a(s))v\cos\theta \qquad (-\tfrac{1}{2}\pi < \theta < \tfrac{1}{2}\pi) \tag{1}$$

Here c_{gb} denotes the local mole fraction of solute within the advancing grain boundary, c_a denotes the local mole fraction just in front of the advancing grain boundary, s denotes arc length measured along the grain boundary, v is the (positive) velocity of the grain boundary in the positive y direction (the y axis being taken parallel to the faces of the foil, as shown in Fig. 1) and θ is the angle between the grain boundary and the positive x-axis, which is taken to be perpendicular to the face of the foil. The local mole fraction in the grain left behind by the advancing grain boundary is equal to c_{gb}

[1] For some existence and uniqueness results about the equations of this model, see ref. [4].

[2] For a detailed analysis of this interaction, arising out of discussions at the conference between J Ockendon and one of the authors, see ref.[13].

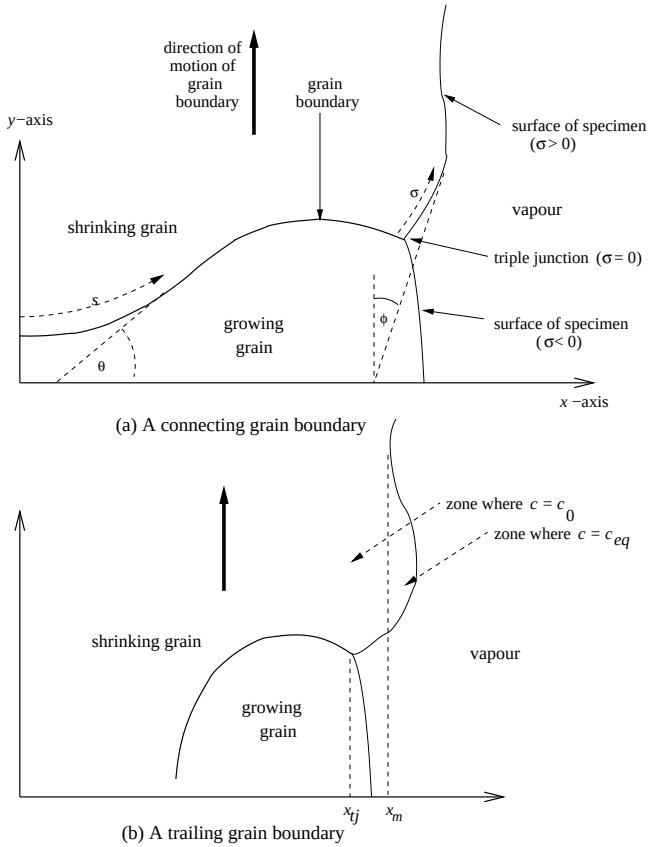

FIGURE 1. The two types of steadily moving grain boundary and the notation used in this paper. In this paper we solve the trailing case. Arc length in the grain boundary is denoted by s; in the solid-vapour surface, by σ (with $\sigma > 0$ in the shrinking grain, $\sigma < 0$ in the growing grain). The angle between the grain boundary and the x-axis is denoted by θ; the angle between the solid-vapour interface and the y-axis, by ϕ.

Usually c_a is equal to c_0, the concentration in the shrinking grain well ahead of the moving grain boundary, but near the surface there can be a thin zone in which the metal in front of the grain boundary arrived there as a result of deposition from the vapour; in this zone, c_a is approximately equal to c_{eq}, the concentration of solute at a flat interface in equilibrium with the vapour. Let x_m be the smallest local minimum value of x reached by the surface of the shrinking grain at points other than the triple junction, and let x_{tj} be the x-coordinate of the triple junction. If $x_m > x_{tj}$ (as is the case in Fig.1(b)) then the zone, if it exists, does not meet the

grain boundary, but if $x_m \le x_{tj}$ then its inner boundary meets the grain boundary at a point whose x-coordinate is x_m. The rule determining c_a can be written

$$c_a = \begin{cases} c_0 & \text{if} \quad 0 \le x < \min(x_m, x_{tj}), \\ c_{eq} & \text{if} \quad x_m < x < x_{tj}. \end{cases} \tag{2}$$

The second differential equation, expressing the local normal velocity $v\cos\theta$ of the grain boundary in terms of the elastic driving force and the surface tension force due to the curvature of the grain boundary, is

$$v\cos\theta = d\theta/ds + \epsilon(c_{gb} - c_a)^2 \qquad \text{if } -\tfrac{1}{2}\pi < \theta < \tfrac{1}{2}\pi, \tag{3}$$

where

$$\epsilon := Y\eta^2 D\lambda/M\gamma^2 \tag{4}$$

is a dimensionless constant measuring the strength of the elastic interaction driving the DIGM. In this definition, Y is a certain elastic modulus, η is the rate of change of stress-free lattice spacing with respect to changes in mole fraction, D is the diffusivity in the grain boundary, λ is its thickness, M is its mobility (velocity per unit driving pressure) and γ is its energy per unit area.

The units of measurement have been chosen so that $D\lambda = 1$ and also $M\gamma = 1$. In a general system of units, s would be replaced by $(D\lambda/M\gamma)s$ and v by $[(M\gamma)^2/D\lambda]v$, but the formula (4) would not change. Although the values of both D and M are not known with any accuracy for real metals and are expected to vary greatly with composition and with temperature (as an Arrhenius exponential of the reciprocal of temperature) only their ratio, which is less sensitive to temperature, appears in (4); hence the order of magnitude of ϵ can be estimated from theory or experiment. Nevertheless, since η can vary widely (from near zero in silver-gold to 0.15 in nickel-gold) we expect ϵ also to vary widely. In the present paper we investigate the behaviour of this mathematical model in the limit of very small ϵ.

Eqns (1) - (3) are given here only in the form they take when $-\frac{1}{2}\pi < \theta < \frac{1}{2}\pi$ on the whole of the grain boundary. For values of θ outside this range the equations are different, reflecting the possibility of the grain boundary's passing a point in the metal more than once; this generalization is considered in section 8.

The solutions of eqns (1) and (3) satisfy boundary conditions at each end of the curve. One of these ends is the triple junction shown in Fig. 1, at which the grain boundary meets the external surfaces of the two crystal grains. For connecting grain boundaries, the other end is a similar triple junction at the corresponding point on the other side of the mid-plane of the foil. Assuming that the grain boundary is symmetrical about this plane, the concentration will be an even function of displacement from this plane and the angle will be an odd function, so that we need only consider one half of the grain boundary only, with suitable conditions at the mid-point, which we also take as the origin of the arc length coordinate s:

$$\left.\begin{aligned} \theta &= 0 \\ dc_{gb}/ds &= 0 \end{aligned}\right\} \tag{5}$$

For trailing grain boundaries, there is no symmetry, but instead there are conditions in the far distance behind the triple junction, namely

$$\left.\begin{array}{rcl} \theta & \rightarrow & \frac{1}{2}\pi \\ c_{gb} - c_a & \rightarrow & 0 \end{array}\right\} \tag{6}$$

where the location of the point at which $s = 0$ is now arbitrary.

In addition to the condition (5) or (6) there are two conditions at the triple junction itself. These conditions are the same for both cases. One of them (arising from the requirement that the chemical potentials must be continuous at the triple junction) can be written

$$c_{tj} = c_{eq} \tag{7}$$

where c_{tj} denotes the value of c_{gb} at the triple junction and c_{eq} is defined above. By varying the partial pressure of solute atoms in the vapour, the experimenter can control the value of c_{eq} and hence that of c_{tj}. The second boundary condition concerns the direction of the tangent to the grain boundary at the triple junction, *i.e.,* the value of $\theta_{tj} := \theta(s_{tj})$ where s_{tj} denotes the value of s at the triple junction. In refs [2, 5] the simplest possible approximation was used, namely that the grain boundary is perpendicular to the surface (i.e. $\theta_{tj} = 0$), but this approximation can obscure some interesting effects. To complete the specification of the boundary conditions, we need a condition from which θ_{tj} can be determined; this condition is considered in the following section.

3. The Mullins theory for surface motion by surface diffusion

In the presence of a grain boundary the surface of the specimen is not flat because there is a groove at the triple junction, where the angles are determined by the surface tensions (free energies per unit area) of the three interfaces meeting there. The resulting curvature affects the chemical potential at the surface, and gradients in this chemical potential cause matter to diffuse along the surface so that it is deposited in some places and removed from others.

A theory of this surface motion by diffusion in the case of a pure substance was developed by Mullins[10]. According to his ideas, the chemical potential varies linearly with the curvature, the material flux along the surface is proportional to the gradient of the chemical potential, and the deposition rate on the surface is minus the surface divergence of the flux; the resulting local normal velocity of the surface is therefore proportional to minus the surface Laplacian of surface curvature, in our case $d^3\phi/d\sigma^3$ where σ is arc length along the surface and ϕ is the angle between the surface and the y axis. If the surface profile of the metal moves like a wave travelling in the y direction with velocity v, this local deposition rate is $-v \sin\phi$, and so ϕ satisfies the differential equation

$$b\, d^3\phi/d\sigma^3 = v \sin\phi \tag{8}$$

where b is a dimensionless material constant. In a general system of units, b would be replaced by the material constant B used by Mullins, which has dimensions

(length)^4 (time)$^{-1}$ and is related to b by the formula $B = b(D\lambda)^2/(M\gamma)$. Eq (8), which was given by Kanel, Novick-Cohen and Vilenkin [12], is the nonlinear generalization of an equation formulated by Mullins[11], which in our notation would read $b\,d^4x/dy^4 = v\,dx/dy$.

In ref. [11] Mullins found that the end of the moving grain boundary would make a fixed angle with the x axis, independent of the speed v (though it would change sign if the sign of v were reversed). His result can be written

$$\theta_{tj} = -\tfrac{1}{6}\delta \tag{9}$$

where δ is the discontinuity in ϕ, which is determined by the surface tension equilibrium at the triple junction. One of the results of the present paper is a generalization of (9), eqn (35) below. The extra term on the left side of (35) arises from the nonlinearity of eqn (8). The right side of (35) would be replaced by zero for the problems considered by Mullins and by Kanel et al.; this term arises from a further effect which we now consider.

Eqn (8) was formulated for a pure substance in equilibrium with its vapour. Here, however, we are concerned with an alloy whose concentration may vary along the surface. Furthermore the formulation of the boundary condition at the triple junction has to be amended to take account of flow into and out of the grain boundary. The relevant generalization of Mullins' theory has been considered by Brener and Temkin [1], who (using the same linearization approximation as Mullins[11]) obtain a pair of equations for the fluxes of both types of atom along the surface. The present paper applies to an alloy (*e.g.* iron-zinc) where the solute (zinc) is volatile while the solvent (iron) can be assumed non-volatile, in which case only one equation is necessary; for a travelling wave the equation is [3]

$$b(1-c_{eq})\,d^3\phi/d\sigma^3 = (1-c_a)v\sin\phi \tag{10}$$

where c_a means essentially the same thing as in eqn (1), i.e. $c_a = c_0$ at points which the surface is passing for the first time, and $c_a = c_{eq}$ if the surface has been there before. In the rest of this paper we confine ourselves to the case where c_{eq} and c_0 are close enough together to justify treating the factors $1-c_{eq}$ and $1-c_{de}$ as equal, so that (8) can be used in place of (10).

The boundary conditions on (8) at infinity are, naturally,

$$\phi(\sigma) \to 0 \text{ as } \sigma \to \pm\infty \tag{11}$$

At the triple junction (where we take $\sigma = 0$) the function $\phi(\sigma)$ is discontinuous. The angles there are related to each other and to the angle at the end of the grain boundary by

$$\begin{aligned} \phi(+0) - \phi(-0) &= \delta \\ \phi(+0) + \phi(-0) &= -2\theta_{tj} \end{aligned} \tag{12}$$

where in the second line we have assumed that the surface tensions of the two external surfaces are equal, so that at the triple junction the tangent to the grain boundary bisects the angle between the tangents to the two external surfaces. A

second condition comes from requiring the chemical potential of the solute to be continuous at the triple junction; since this chemical potential depends on the curvature, the condition is

$$\phi'(+0) = \phi'(-0) \tag{13}$$

where the prime attached to ϕ denotes a derivative.

Finally, there is a condition arising from the fact that matter is conserved at the triple junction, so that the algebraic sum of the flows of solvent in the three surfaces meeting there is zero. Since the flows in the outer surfaces are proportional to the gradient of the curvature ϕ' while that in the grain boundary is proportional to the gradient of the concentration there, the conservation condition can be shown[3] to take the form

$$\phi''(+0) - \phi''(-0) = b^{-1} c'_{tj}. \tag{14}$$

where c'_{tj} denotes the value of dc_{gb}/ds at the outer end of the grain boundary, i.e. at the triple junction. In a general system of units the coefficient b^{-1} would be replaced by $M\gamma/D\lambda b = D\lambda/B$ where B is the material constant mentioned earlier, which is defined in Mullins' papers[10, 11].

For the problem considered in refs [11, 12], there is no flow of matter along the grain boundary, and so the right side of (14) is replaced there by 0.

4. Analysis of the nonlinear surface diffusion equation

In the phase space of the differential equation (8) there is a fixed point at $(\phi, \phi', \phi'') = (0, 0, 0)$. Near this fixed point the equation can be approximated as the linear system $(d/d\sigma)[\phi, \phi', \phi'']^T = A[\phi, \phi', \phi'']^T$ where T denotes a transpose and A is the matrix

$$A := \begin{bmatrix} 0 & 1 & 0 \\ 0 & 0 & 1 \\ v/b & 0 & 0 \end{bmatrix} \tag{15}$$

The expanding subspace of this fixed point is one-dimensional and is spanned by the vector $(1, \alpha, \alpha^2)^T$ where $\alpha := (v/b)^{1/3}$, so that on it we have $\phi' = \alpha\phi, \phi'' = \alpha^2\phi$. The corresponding expanding manifold can be (locally) parametrized by the variable ϕ : in some neighbourhood of the fixed point the other two coordinates can be expressed as power series in ϕ whose linear terms correspond to the linearized solution, namely

$$\phi' = \alpha\phi[1 - \tfrac{1}{78}\phi^2 + \tfrac{79}{628680}\phi^4 - \tfrac{1021}{6521926320}\phi^6 + \dots] \tag{16}$$

$$\phi'' = \alpha^2\phi[1 - \tfrac{2}{39}\phi^2 + \tfrac{98}{78585}\phi^4 - \tfrac{5764}{407620395}\phi^6 + \dots] \tag{17}$$

These series were computed by requiring them to satisfy the equations $\phi' d\phi'/d\phi = \phi'', \phi' d\phi''/d\phi = \alpha^3 \sin\phi$

The contracting subspace of the fixed point is two-dimensional, being spanned by the real and imaginary parts of the vector $(1, \alpha\omega, \alpha^2\omega^2)$ where ω is either of the complex cube roots of 1. Since $1 + \omega + \omega^2 = 0$, any vector (ϕ, ϕ', ϕ'') in the

subspace satisfies $\alpha^2\phi + \alpha\phi' + \phi'' = 0$. The corresponding contracting manifold can be locally parametrized by the pair ϕ, ϕ'; in some neighbourhood of the fixed point the remaining coordinate ϕ'' can be expressed as a power series in these parameters whose linear term corresponds to the linearized solution:

$$\phi'' = -p - q + \tfrac{23}{273}p^3 + \tfrac{15}{182}p^2q + \tfrac{4}{91}pq^2 + \tfrac{1}{91}q^3 - \tfrac{125663}{73162635}p^5 \qquad (18)$$
$$+\tfrac{12793}{39020072}p^4q + \tfrac{36256}{14632527}p^3q^2 + \tfrac{3495}{1393574}p^2q^3 + \tfrac{5961}{4877509}pq^4 + \tfrac{184}{696787}q^5 + \dots$$

where $p := \alpha^2\phi, q := \alpha\phi'$. This series was computed by requiring it to satisfy $\phi'\partial\phi''/\partial\phi + \phi''\partial\phi''/\partial\phi' = \alpha^3 \sin\phi$.

5. The matching condition at the triple junction

For the shrinking grain, σ is positive and the function $\phi(\sigma)$ satisfies the boundary condition (11) for $\sigma \to +\infty$; it therefore belongs to the contracting manifold and satisfies (18). For the growing grain, σ is negative and the function $\phi(\sigma)$ satisfies the boundary condition (11) for $\sigma \to -\infty$; it therefore belongs to the expanding manifold and satisfies (16), (17). The two second derivatives in (14) can therefore be written

$$\begin{array}{lrcll} \text{shrinking grain :} & \phi''(+0) & = & -\alpha^2\phi(+0) - \alpha\phi'(+0) + \dots & \text{by (18)} \\ & & = & -\alpha^2\phi(+0) - \alpha\phi'(-0) + \dots & \text{by (13)} \\ & & = & -\alpha^2\phi(+0) - \alpha^2\phi(-0) + \dots & \text{by (16)} \\ \text{growing grain :} & \phi''(-0) & = & \alpha^2\phi(-0) + \dots & \text{by (17)} \end{array} \qquad (19)$$

so that (14) itself becomes

$$\begin{aligned} b^{-1}c'_{tj} &= \phi''(+0) - \phi''(-0) \\ &= -\alpha^2\phi(+0) - 2\alpha^2\phi'(-0) + \dots \end{aligned} \qquad (20)$$

Using (12), which implies $\phi(\pm 0) = -\theta_{tj} \pm \frac{1}{2}\delta$, we can write (20) in the form

$$b^{-1}\alpha^{-2}c'_{tj} = 3\theta_{tj} + \tfrac{1}{2}\delta + H(\theta_{tj}, \delta) \qquad (21)$$

where the higher terms in the series are incorporated in the function

$$H(\theta, \delta) := -\tfrac{2}{7}\theta^3 + \tfrac{3}{91}\theta^2\delta - \tfrac{8}{91}\theta\delta^2 - \tfrac{1}{273}\delta^3 + O(|\theta|^5 + |\delta|^5) \qquad (22)$$

6. Solving the equations

Only trailing grain boundaries will be studied in this paper. The connecting grain boundaries will be considered in a forthcoming paper[3]. To simplify the notation we write $c(s)$ or c in place of $c_{gb}(s)$ from here on.

The problem we consider is to find the speed v of the trailing grain boundary for a given value of the experimentally controllable parameter $\Delta c := c_{eq} - c_0$, which lies in the interval $[-1, +1]$. Our method is to find a family of solutions for eqns (1) and (3) satisfying the boundary condition (6), treating v as a parameter.

Then we pick out the solution and the value of v so that the boundary conditions (7) and (21) are satisfied.

We shall make the approximation of assuming that $x_{tj} - x_m$, if positive, is negligibly small, so that (2) simplifies to $c_a = c_0$; this assumption will be justified *a posteriori* — see the discussion of eqn (40). It is convenient also to introduce the new variable $\psi := \frac{1}{2}\pi - \theta$, so that eqns (1), (3) become

$$d^2c/ds^2 = (c - c_0)v \sin\psi \tag{23}$$

$$d\psi/ds = \epsilon(c - c_0)^2 - v \sin\psi \qquad \text{if } 0 < \psi < \pi) \tag{24}$$

with the boundary conditions $c \to c_0, dc/ds \to 0, \psi \to 0$ as $s \to -\infty$. In the range where $0 < \psi < \pi$, the order of the system can be reduced to two by going over to ψ as independent variable:

$$(\epsilon(c - c_0)^2 - v \sin\psi)\frac{\partial}{\partial\psi}\left[(\epsilon(c - c_0)^2 - v \sin\psi)\frac{\partial c}{\partial\psi}\right] = (c - c_0)v \sin\psi \tag{25}$$

with the boundary conditions $c \to c_0, [\epsilon(c - c_0)^2 - v \sin\psi]dc/d\psi \to 0$ as $\psi \to 0$.

The solutions of eqn (25) depend on the material parameter ϵ as well as on the experimentally controllable parameter Δc. We shall look for a linkage between these two parameters which leads to a family of solutions which are asymptotically self-similar in the limit $\epsilon \to 0$. To do this, we seek solutions whose asymptotic behaviour in this limit is

$$\left.\begin{array}{rcl} c(\psi) - c_0 & \sim & \epsilon^m \hat{c}(\psi) \\ v & \sim & \epsilon^n \hat{v} \end{array}\right\} \quad \text{as} \quad \epsilon \to 0 \tag{26}$$

where m and n are constants, to be chosen later so that a useful self-similar family is obtained. To begin the process of choosing m and n, let us require

$$2m + 1 < n; \tag{27}$$

then it follows that $v \sin\psi$ becomes negligible in comparison with ϵc^2 as $\epsilon \to 0$, so that (25) simplifies to

$$\epsilon^{2+4m}\hat{c}\frac{d}{d\psi}\left(\hat{c}^2\frac{d\hat{c}}{d\psi}\right)(1 + o(1)) = \epsilon^n \hat{v} \sin\psi \tag{28}$$

with the boundary conditions $\hat{c} \to 0, \hat{c}^2 d\hat{c}/d\psi \to 0$ as $\psi \to 0$. To obtain a useful result, we require

$$2 + 4m = n \tag{29}$$

so that eqn (28) simplifies further to

$$\hat{c}\frac{d}{d\psi}\left(\hat{c}^2\frac{d\hat{c}}{d\psi}\right) = \hat{v} \sin\psi \tag{30}$$

The solution of this equation satisfying the boundary conditions at $\psi = 0$ can be computed as a series or by numerical integration. The series solution is

$$\hat{c} = \pm\left(\frac{16\hat{v}}{15}\right)^{1/4}\psi^{3/4}[1 - \tfrac{5}{472}\psi^2 + \tfrac{511}{6683520}\psi^4 + \tfrac{66797}{357734071296}\psi^6 + \dots] \tag{31}$$

To apply the concentration condition at the triple junction, eqn (7), we first evaluate (31) at the triple junction, obtaining

$$\hat{c}_{tj} = \pm \left(\frac{16\hat{v}}{15}\right)^{1/4} \psi_{tj}^{3/4}[1 - \tfrac{5}{472}\psi_{tj}^2 + \dots] \tag{32}$$

where $\psi_{tj} := \frac{1}{2}\pi - \theta_{tj}$ is the value of ψ at the triple junction and $\hat{c}_{tj}$ is defined, in analogy with (26), by $c_{tj} - c_0 = \epsilon^m \hat{c}_{tj}$. Then (7) becomes $c_{eq} - c_0 = \epsilon^m \hat{c}_{tj}$, i.e.

$$\Delta c = \epsilon^m \hat{c}_{tj}. \tag{33}$$

To apply the triple junction angle condition (21), we need a formula for dc/ds; eqns (24), (26) and (31) give the asymptotic result

$$\frac{dc}{ds} = [\epsilon(c - c_0)^2 - v\sin\psi]\frac{dc}{d\psi} \sim \epsilon^{3m+1}\hat{c}^2\frac{d\hat{c}}{d\psi} = \pm\frac{3\epsilon^{3m+1}}{4}\left(\frac{16\hat{v}}{15}\right)^{3/4}\psi^{5/4}\times$$

$$\times[1 - \tfrac{85}{1416}\psi^2 + \tfrac{6305}{4010112}\psi^4 - \tfrac{7198697}{357734071296}\psi^6 + \dots]. \tag{34}$$

The sign in (34) is the same as that of $c - c_0$. When (34) is substituted into the triple junction angle condition (21), using also (26), the result is

$$3\theta_{tj} + \tfrac{1}{2}\delta + H(\theta_{tj}, \delta) = b^{-1}(v/b)^{-2/3}c'_{tj}$$

$$= \pm b^{-1/3}(\epsilon^n\hat{v})^{-2/3}\frac{3\epsilon^{3m+1}}{4}\left(\frac{16\hat{v}}{15}\right)^{3/4}\psi_{tj}^{5/4}[1 - \tfrac{85}{1416}\psi_{tj}^2 + \dots](1 + o(1)). \tag{35}$$

To make eqn (35) approach a useful limit as $\epsilon \to 0$, we require the right side to be formally independent of ϵ, *i.e.,*

$$-2n/3 + 3m + 1 = 0 \tag{36}$$

Then (35) simplifies (after dividing by 3 and taking the limit $\epsilon \to 0$) to

$$\theta_{tj} + \tfrac{1}{6}\delta + \tfrac{1}{3}H(\theta_{tj}, \delta)$$

$$= \pm\frac{b^{-1/3}}{4}\left(\frac{16}{15}\right)^{3/4}\hat{v}^{1/12}\psi_{tj}^{5/4}[1 - \tfrac{85}{1416}\psi_{tj}^2 + \dots] \tag{37}$$

where the sign is the same as that of $\hat{c}_{tj}$. The solution of eqns (29), (36) is $m = 1, n = 6$, and these numbers also satisfy (27). Thus we can now be more specific about the ansatz (26) and the formula (33), replacing them by

$$\left.\begin{array}{rcl} c(\psi) - c_0 & \sim & \epsilon\hat{c}(\psi) \\ v & \sim & \epsilon^6\hat{v} \end{array}\right\} \quad \text{as} \quad \epsilon \to 0$$

$$\Delta c = \epsilon\hat{c}_{tj} \tag{38}$$

From these formulas we can obtain information about the sizes of the structures under study. The growing crystal grain forms a thin layer under the surface

of the specimen. Its thickness is the sum of two parts; one part is the depth of its inner surface below the triple junction, given by

$$\begin{aligned} h_1 &:= \int_{-\infty}^{s_{tj}} \cos\theta \, ds = \int_0^{\psi_{tj}} \frac{\sin\psi \, d\psi}{\epsilon(c-c_0)^2 - v\sin\psi} && \text{by (24)} \\ &\sim \frac{1}{\epsilon^3} \int_0^{\psi_{tj}} \frac{\sin\psi \, d\psi}{\hat{c}^2} && \text{by (38)} \\ &= \frac{1}{\epsilon^3} \left(\frac{15}{16\hat{v}}\right)^{1/2} \int_0^{\psi_{tj}} \frac{\sin\psi \, d\psi}{\psi^{3/2}[1 - \frac{5}{472}\psi^2 + \dots]^2}, && (39) \end{aligned}$$

by (31). The other contribution is the depth of the triple junction below the surface of the shrinking grain, given by

$$\begin{aligned} h_2 &:= -\textstyle\int_{-\infty}^{0} \sin\phi(\sigma) \, d\sigma \\ &= -(b/v) \textstyle\int_{-\infty}^{0} d^3\phi/d\sigma^3 \, d\sigma && \text{by (8)} \\ &= -(b/v)\phi''(-0) \\ &= -(b/v)(\alpha^2\phi(-0) + \dots) && \text{by (19)} \\ &= (b/v)^{1/3}(\theta_{tj} + \tfrac{1}{2}\delta + \dots) && \text{by (12)} \\ &\sim \epsilon^{-2}(b/\hat{v})^{1/3}(\theta_{tj} + \tfrac{1}{2}\delta + \dots) && \text{by (38)} \end{aligned} \qquad (40)$$

Since ϵ is small, the contribution h_1 dominates, and the thickness of the growing layer is of order ϵ^{-3}. Obviously this must be less than the overall thickness of the specimen, so it is a necessary condition for the applicability of these results that the thickness of the specimen should be of order ϵ^{-3} or greater. If the specimen is thinner than this, then DIGM is possible, if at all, only for connecting grain boundaries, which are outside the scope of this paper.

Formula (40) shows that the depth of the triple junction below the surface of the growing crystal is of order ϵ^{-2}. The sizes of other features of the outer boundary such as the depth of the triple junction below the surface of the growing crystal, the difference in thickness of the two crystals, and the thickness of the zone comprising the parts of the shrinking crystal that are deposited from the vapour as the grain boundary advances, are likewise of order ϵ^{-2}. From this it follows that $x_{tj} - x_m = O(\epsilon^{-2}) \ll x_{tj} = O(\epsilon^{-3})$, justifying our neglect of $x_{tj} - x_m$ in setting up eqn (23).

7. The speed of DIGM

To complete the calculation we want to find $\hat{v}$, which determines the speed of the grain boundary and enters into the formula (31) for $\hat{c}(\psi)$ from which the shape and size of the grain boundary can be calculated. We treat $\hat{c}_{tj}$ as known (from (4) and (38)), so it is a question of solving the pair of equations (32) and (37) for the two unknowns $\hat{v}$ and ψ_{tj}. A reasonably accurate method of solution is first to take the cube root of (32) and eliminate $v^{1/12}$ between the resulting equation and (37)

to obtain

$$(K\hat{c}_{tj})^{1/3} = \frac{F(\psi_{tj},\delta)}{\psi_{tj}} \tag{41}$$

where

$$K := \frac{4}{225b} \tag{42}$$

$$F(\psi_{tj},\delta) := [\tfrac{1}{2}\pi - \psi_{tj} + \tfrac{1}{6}\delta + \tfrac{1}{3}H(\tfrac{1}{2}\pi - \psi_{tj},\delta)]\frac{[1-\frac{5}{472}\psi_{tj}^2+\dots]^{1/3}}{[1-\frac{85}{1416}\psi_{tj}^2+\dots]} \tag{43}$$

As ψ_{tj} increases over its allowed range $[0,\pi]$ at fixed δ the right side of (41) decreases monotonically from $+\infty$ to a negative value $F(\pi,\delta)/\pi$. Eqn (41) therefore has a unique solution for ψ_{tj} provided that $(K\hat{c}_{tj}) \geq -|F(\pi,\delta)/\pi|^3$. The value of $|F(\pi,\delta)/\pi|^3$ varies from $(0.671\dots)^3 = 0.302\dots$ at $\delta = 0$ to $(0.181\dots)^3 = 0.0059\dots$ at $\delta = \pi$.

An estimate of the value of $\hat{v}$ for a given $\hat{c}_{tj}$ can be derived from the following (unproved) bounds, which were obtained from graphs of $F(\psi_{tj},\delta) - \frac{1}{6}\delta$ against ψ_{tj} for various δ:

$$0.35 - 0.8\psi_{tj} < F(\psi_{tj},\delta) - \tfrac{1}{6}\delta < 1.5 - 0.8\psi_{tj} \tag{44}$$

Using these in (41) and solving for ψ_{tj} we find

$$\psi_{tj} = \frac{N_1 + \frac{1}{6}\delta}{0.8 + (K\hat{c}_{tj})^{1/3}} \tag{45}$$

where $0.35 < N_1 < 1.5$.

Solving (32) for $\hat{v}$ and then using (45) together with the fact that $0.903 < [1 - \frac{5}{472}\psi_{tj}^2 + \dots] \leq 1$, we obtain

$$\begin{aligned} \hat{v} &= \frac{15\hat{c}_{tj}^4}{16\psi_{tj}^3}[1-\tfrac{5}{472}\psi_{tj}^2+\dots]^{-4} \\ &= \frac{15\hat{c}_{tj}^4}{16}\left(\frac{0.8+(K\hat{c}_{tj})^{1/3}}{N_1+\frac{1}{6}\delta}\right)^3 N_2 \\ \text{i.e. } v &= \frac{15N_2\epsilon\Delta c^4}{16}\left(\frac{0.8\epsilon^{1/3}+(K\Delta c)^{1/3}}{N_1+\frac{1}{6}\delta}\right)^3(1+o(1)) \end{aligned} \tag{46}$$

where $1 \leq N_2 \leq (0.903)^{-4} = 1.504\dots$. Thus, provided always that $K\hat{c} \geq -|F(\pi,\delta)/\pi|^3$, the speed of trailing DIGM is approximately quadratic in ϵ and proportional to the fourth power of the applied concentration difference Δc when Δc is small (compared with $(0.8)^3\epsilon/K$), but linear in ϵ and proportional to the fifth power of Δc, when Δc is large and positive.

Besides the speed, we can also calculate the thickness of the trailing layer. To leading order the thickness is given by (39) as $\hat{v}^{-1/2}$ times an increasing function of ψ_{tj} which is approximately proportional to $\psi_{tj}^{1/2}$ at small ψ_{tj} and

approaches a constant as $\psi_{tj} \to \pi$. Consequently, by (45) and (46), the thickness is approximately proportional to $\epsilon^{-3}\hat{c}_{tj}^{-2} = \epsilon^{-1}(\Delta c)^{-2}$ at small Δc, and to $\epsilon^{-3}\hat{c}_{tj}^{-5/2}\hat{c}_{tj}^{-1/6} = \epsilon^{-3}\hat{c}_{tj}^{-8/3} = \epsilon^{-1/3}(\Delta c)^{-8/3}$ at large Δc.

8. Generalizing the equations of the model

To treat the case $K\hat{c} < -|F(\pi,\delta)/\pi|^3$ we need to generalize the fundamental equations of our model to values of θ outside the range $-\frac{1}{2}\pi < \theta < \frac{1}{2}\pi$ used in (1) and (3). The new possibility is that $\cos\theta$ may be negative, describing a section of grain boundary along which s increases to the left instead of the right, so that the moving grain boundary may be traversing material points that it has already passed before. The formulation of the equations for such points does not involve any new (local) physics, just rewriting the old equations in a more general notation.

For points on the grain boundary where $\cos\theta \neq 0$, let us define a local unit vector $\mathbf{n}$ which is normal to the grain boundary and makes an acute angle with the positive y-axis. Because we are assuming a travelling wave, the local direction of motion of the grain boundary is in the direction of $\mathbf{n}$, and its normal velocity in this direction is the positive quantity $v|\cos\theta|$. The extension of (1) to general values of θ is therefore

$$\frac{d^2 c_{gb}}{ds^2} = (c_{gb}(s) - c_a(s))v|\cos\theta|, \tag{47}$$

where c_a, as before, represents the mole fraction c just in front of the moving grain boundary. If the relevant material point has not been passed before by the grain boundary, c_a is given by eqn (2); otherwise it is equal to the value of c_{gb} at the same value of x for the most recent previous passing, that is $c_a(x,y) = c_{gb}(x,y_1)$ for the smallest $y_1 > y$ at which (x,y_1) is on a grain boundary. Eqn (47) can also be used at the places where $\cos\theta = 0$ since the normal velocity there is zero regardless of the direction chosen for the unit normal vector.

The generalized force balance equation says that the normal velocity $v|\cos\theta|$ equals the sum of the curvature force and the elastic driving force, both reckoned as positive if they are in the direction of the above unit normal vector. The curvature force is $d\theta/ds$ in the direction of more usual normal vector which is on the left of a person walking along the curve in the direction of increasing s. This more usual normal vector is equal to $\mathbf{n}S(\theta)$, where

$$S(\theta) := \begin{cases} +1 & \text{if} \quad \cos\theta > 0 \\ -1 & \text{if} \quad \cos\theta < 0. \end{cases} \tag{48}$$

Therefore the curvature force in the direction of $\mathbf{n}$ is $S(\theta)d\theta/ds$. The elastic driving force always acts in the direction of motion, and is therefore positive under our sign convention and is given by the same expression as in (3). Combining the three terms, we obtain the following generalization of the force balance equation (3)

$$v|\cos\theta| = S(\theta)d\theta/ds + \epsilon(c_{gb}(s) - c_a(s))^2 \text{ if } \cos\theta \neq 0. \tag{49}$$

Here c_a, as in (47), denotes the concentration just in front of the advancing grain boundary. An equivalent form for (49), which we shall refer to later, is

$$d\theta/ds = v\cos\theta - \epsilon(c_{gb}(s) - c_a(s))^2 S(\theta) \text{ if } \cos\theta \neq 0. \tag{50}$$

Unlike (47), eqn (49) cannot be used at the places where $\cos\theta = 0$; at such places the normal velocity of the grain boundary is zero and so the elastic force on the grain boundary is not given by the formula $\epsilon(c_{gb}(s) - c_a(s))^2$, which applies only when the normal velocity is non-zero. Nevertheless, if we include the natural stipulation that (so as to exclude kinks) θ must vary continuously with s, eqn (49) does make a clear prediction about what happens at places where $\cos\theta = 0$, provided also that $\sin\theta < 0$ there. To obtain this prediction, note that eqn (49) implies, whenever $\cos\theta \neq 0$,

$$\begin{aligned} \frac{d}{ds}|\cos\theta| &= S(\theta)\frac{d}{ds}\cos\theta \\ &= -\sin\theta\{v|\cos\theta| - \epsilon(c_{gb} - c_a)^2\} \text{ by (49)} \\ &\leq v|\cos\theta| + \epsilon\sin\theta(c_{gb} - c_a)^2 \end{aligned} \tag{51}$$

If we define $f(s) := \mathrm{e}^{-vs}|\cos\theta(s)|$, it follows that $df/ds \leq 0$ whenever $\cos\theta \neq 0$ and $\sin\theta < 0$. Now let s_0 be some value of s at which $\theta = -\frac{1}{2}\pi$. At this value we have $f(s) = 0$ and $\sin\theta(s) < 0$, and it follows[3] from the non-positivity of df/ds that $f(s) = 0$ for all $s > s_0$, and hence that θ remains at the value $-\frac{1}{2}\pi$ for all $s > s_0$.

This is a puzzling result. The model predicts that the grain boundary can have a straight part, as illustrated in Fig.2, on which there is no normal velocity and no curvature; yet the mole fractions at nearby points on the two sides of the straight part are different, which leads one to expect an elastic force on it, in violation of the force balance principle used to derive (49). Mathematically, the difficulty is related to the singular character of the differential equation (50), whose right side is not a continuous function of s as $\cos\theta$ passes through the value $-\frac{1}{2}\pi$. The way round the paradox may be connected with stability; for although the result shows that the straight section of the grain boundary is stable against small perturbations within the class of travelling wave solutions, it does not prove stability against perturbations which are outside this class. The theory of these more general perturbations, in which the shape of the curve in Fig. 2 would depend on time, is outside the scope of this paper; all we do here is to work out the travelling wave solution from which such a stability analysis would start.

9. Predictions of the model for the case $K\hat{c} < -|F(\pi, \delta)/\pi|^3$

The result just derived implies that the grain boundary consists of two distinct parts, as illustrated in Fig.2 : a curved inner part on which $\theta > -\frac{1}{2}\pi$, smoothly

[3]If there were an $s_2 > s_0$ with $f(s_2) > 0$, then by the continuity of $\theta(s)$ there would be an s_1 satisfying $s_0 < s_1 < s_2$ with $0 = f(s_0) < f(s_1) < f(s_2)$, but this last inequality is incompatible with the non-positivity of df/ds when $\cos\theta \neq 0$.

joined to a straight outer part, parallel to the faces of the crystal, on which $\theta = -\frac{1}{2}\pi$. The outer straight part would be a solution to (50) if the last term were set to 0 by assumption when $\cos\theta = 0$.

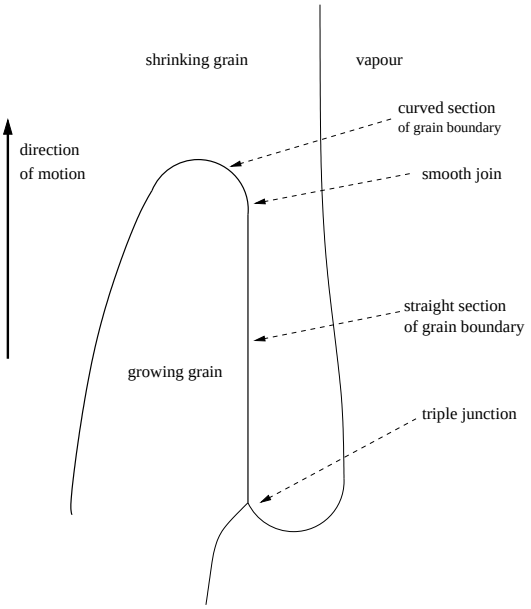

FIGURE 2. Sketch of the grain boundary when $\Delta c < -(\epsilon/K|F(\pi,\delta)/\pi|^3$

On the straight part, eqn (47) is simply

$$d^2c/ds^2 = 0. \tag{52}$$

At the smooth join $c, dc/ds$ and ψ are continuous; let us denote their values there by c_{sj}, c'_{sj} and ψ_{sj}. Then eqn (52) tells us that

$$\begin{aligned} c(s) &= c_{sj} + (s - s_{sj})c'_{sj} \\ c_{tj} &= c_{sj} + (s_{tj} - s_{sj})c'_{sj} \\ c'_{tj} &= c'_{sj} \neq 0 \end{aligned} \tag{53}$$

For the curved part of the grain boundary the method of solving the equations is nearly the same as in section 6; the only difference is that the places of c_{tj}, c'_{tj} and ψ_{tj} are now taken by c_{sj}, c'_{sj} and $\psi_{sj} = \pi$. The analogue of (41) can be written

$$\hat{c}_{sj} = \frac{1}{K}\left(\frac{F(\pi,\delta)}{\pi}\right)^3 = -\frac{1}{K}\left|\frac{F(\pi,\delta)}{\pi}\right|^3 \tag{54}$$

Putting this into the analogue of the first line of (46), we obtain

$$\begin{aligned} \hat{v} &= \frac{15\hat{c}_{sj}^4}{16\pi^3[1-\frac{5}{472}\pi^2+\dots]^4} = 0.0455\hat{c}_{sj}^4 \\ &= \frac{0.0455}{K^4}\left(\frac{F(\pi,\delta)}{\pi}\right)^{12} \text{ by (54)} \\ \text{i.e. } v &= \frac{0.0455\epsilon^6}{K^4}\left(\frac{F(\pi,\delta)}{\pi}\right)^{12}(1+o(1)) \end{aligned} \tag{55}$$

Provided Δc is less than the critical value $-(\epsilon/K)|F(\pi,\delta)/\pi|^3$, the velocity is independent of Δc : no matter how large and negative Δc is made, the velocity cannot be increased beyond the value given in (55). In a similar way it can be shown, using (39) and (40), that the thickness of the grain boundary is independent of Δc under these conditions. Increases of $|\Delta c|$ beyond $(\epsilon/K)|F(\pi,\delta)/\pi|^3$ serve only to increase the length of the straight part of the grain boundary, which according to (53) and (54) is the positive quantity

$$s_{tj}-s_{sj} = \frac{(c_0-c_{tj})-(c_0-c_{sj})}{-c'_{sj}} = \frac{|\Delta c|-(\epsilon/K)|F(\pi,\delta)/\pi|^3}{|c'_{sj}|} \tag{56}$$

Apart from the number 0.0455, which comes from the solution of the grain boundary equations, the scaled speed $\hat{v}$ is determined entirely by the non-linear Mullins theory, depending only on the angle δ at the triple junction and on the value of $K = 4/225b$. However, although $\hat{v}$ is independent of $\hat{c}$ it is extremely sensitive to the other parameters, particularly δ : for example, when $\delta = 0$ the coefficient of K^{-4} in equation (55) is 4×10^{-4}, but when $\delta = \pi$ this coefficient is 7×10^{-11} (the smallness of these numbers is deceptive, since K^{-4} could be large.). Moreover, as we have mentioned earlier, the travelling wave solution underlying the derivation of the results in this section may well be unstable against perturbations which, if they move forward in the y direction at all, do so with speed less than v. The stability against such perturbations would presumably get worse as $|\Delta c|$ was made larger, since any localized perturbation would (by (56)) have more time to grow before colliding with the triple junction.

Acknowledgements

We thank Paul Fife and Charles Elliott for help in the formulation of the sharp-interface limit of the phase-field equations, and for information about the properties of these equations and about the connection between this paper and ref. [5]. We also thank Carol Handwerker for helpful information about DIGM experiments, and both her and Geoffrey McFadden for critical reviews of the manuscript. J.C. thanks Heriot-Watt University for hosting a workshop during which this work was initiated. O.P. thanks the Open University for a research grant, the Institut des Hautes Etudes Scientifiques, Bures-sur-Yvette, France and NIST for their hospitality during part of the gestation of the paper, DIMACS at Rutgers University

for financial support during a visit to the USA, and the Royal Society of London for a grant towards travel expenses to Trento. DIMACS is an NSF Science and Technology Center, funded under contract STC-91-1999; it also receives support from the New Jersey Commission on Science and Technology.

References

[1] Brener, E. A. and Temkin, D. E., Theory of diffusion induced grain boundary migration: is mass transport along free surfaces important? Acta Mater., **50**, 1707-1716 (2002).

[2] Cahn, J. W., Fife, P. C., and Penrose, O., A phase-field model for diffusion-induced grain-boundary motion, Acta Mater., **45**, 4397-4413 (1997).

[3] Cahn, J. W. and Penrose, O., in preparation.

[4] Deckelnick, K. and Elliott, C. M., An existence and uniqueness result for a phase-field model of diffusion-induced grain-boundary motion, Proc. Roy. Soc. Edin., **A131**, 1323-1344 (2001).

[5] Fife, P., Cahn, J. W., and Elliott, C. M., A Free Boundary Model for DIGM, Interfaces Free Bound., **3**, 291-336 (2001).

[6] Deckelnick, K., Elliott, C. M., and Styles, V., Numerical diffusion-induced grain boundary motion, Interfaces Free Bound., **3**, 393-414 (2001).

[7] Handwerker, C., Diffusion-induced grain boundary migration in thin films, in *Diffusion Phenomena in Thin Films and Microelectronic Materials*, ed. D. Gupta and P. S. Ho, Noyes Publications, Park Ridge, NJ, (1985) pp. 245-322.

[8] Hillert, M., On the driving force for diffusion induced grain boundary migration, Scripta Metall., **17**, 237-240 (1983).

[9] Hillert, M. and Purdy, G. R., Chemically induced grain boundary motion, Acta Metall., **26**, 333-340 (1977).

[10] Mullins, W. W., Theory of thermal grooving, J. Appl. Phys., **28**, 333-339 (1957).

[11] Mullins, W. W., The effect of thermal grooving on grain boundary motion, Acta Metall., **6**, 414-427 (1958).

[12] Kanel, J., Novick-Cohen, A. and Vilenkin, A., Coupled surface and grain boundary motion : nonclassical traveling wave solutions, Preprint, 2002.

[13] Penrose, O., On the elastic driving force in DIGM, in preparation.

[14] Sulonen, M.S., On the driving force of discontinuous precipitation and dissolution, Acta Metall. **12**, 749-753 (1964).

Department of Mathematics,
Heriot-Watt University,
Riccarton, Edinburgh EH14 4AS,
Scotland, UK
E-mail address: O.Penrose@ma.hw.ac.uk

Materials Science and Engineering Laboratory,
NIST,
Gaithersburg, MD 20899-8555,
USA
E-mail address: john.cahn@nist.gov